

First-principles calculation of the intersublattice exchange interactions and Curie temperatures of full Heusler alloys Ni_2MnX ($\text{X}=\text{Ga}, \text{In}, \text{Sn}, \text{Sb}$)

E. Şaşıoğlu, L. M. Sandratskii and P. Bruno
Max-Planck Institut für Mikrostrukturphysik, D-06120 Halle, Germany
 (Dated: February 2, 2008)

The interatomic exchange interactions and Curie temperatures in Ni-based full Heusler alloys Ni_2MnX with $\text{X}=\text{Ga}, \text{In}, \text{Sn}$ and Sb are studied within the framework of the density-functional theory. The calculation of the exchange parameters is based on the frozen-magnon approach. Despite closeness of the experimental Curie temperatures for all four systems their magnetism appeared to differ strongly. This difference involves both the Mn–Mn and Mn–Ni exchange interactions. The Curie temperatures, T_C , are calculated within the mean-field approximation by solving a matrix equation for a multi-sublattice system. Good agreement with experiment for all four systems is obtained. The role of different exchange interactions in the formation of T_C of the systems is discussed.

PACS numbers: 75.50.Cc, 75.30.Et, 71.15.Mb

I. INTRODUCTION

Much efforts is currently devoted to the search for ferromagnetic materials suitable for application in semiconductor spintronics devices. To allow an efficient spin-injection into semiconductor these materials must satisfy a number of conditions. In particular they must have the Curie temperature noticeably higher than the room temperature, be compatible with the semiconductors used industrially, and possess a very high spin-polarization of the electron states at the Fermi level.¹ Some of the Heusler compounds were found to have half-metallic ground state^{2,3} which is characterized by a 100% carrier spin-polarization.

A feature of other Heusler alloys that is useful for spintronic applications is very small lattice mismatch with widely employed semiconductors (e.g., Ni_2MnIn and InAs).^{4,5,6} Among further prominent physical properties of this class of materials one can mention a martensitic transformation in Ni_2MnGa which takes place below the Curie temperature.⁷ An interesting combination of physical properties makes Heusler alloys the subject of intensive experimental and theoretical investigations which could motivate their use as multifunctional materials in practical applications.^{8,9,10,11,12,13,14}

In the present work we report the theoretical study of the exchange interactions and Curie temperature of four full Heusler compounds Ni_2MnX with $\text{X}=\text{Ga}, \text{In}, \text{Sn}$ and Sb . Experimentally, all of them are ferromagnetic and have similar values of the Curie temperature.²⁰

First important contribution to the density functional theory study of these systems was made in early paper by Kübler *et al.*,¹⁵ where the microscopic mechanisms of the magnetism of Heusler alloys was discussed on the basis of the calculation of the ferromagnetic and antiferromagnetic alignments of the Mn moments. Recently a detailed study of the magnetic interactions in Ni_2MnGa and Ni_2MnAl was reported by Enkovaara *et al.*¹⁶ The authors used the plane spiral configurations and have shown that the Ni sublattice plays important role in the

magnetic properties of the system.

The main purpose of the present work is a detailed study of the exchange interactions in these systems. In particular we report a systematic study of the exchange interaction between atoms of different sublattices and show that pattern of exchange interactions in these systems deviates strongly from the physical picture that can be expected on the basis of the experimental information available. Indeed common crystal structure, similar chemical composition and close experimental values of the Curie temperature make the assumption natural that the exchange interactions in these systems are similar. Our study shows, however, that this assumption is not correct. The exchange interactions vary strongly depending on the X constituent. In particular, the intersublattice interactions change strongly from system to system. We show that different exchange interactions lead, in agreement with experiment, to similar values of the Curie temperatures. We analyze the relation between the properties of the exchange interactions and the Curie temperatures.

The paper is organized as follows. In Sec. II we present the calculational approach. Section III contains the results of the calculations and discussion. Section IV gives the conclusions.

II. CALCULATIONAL APPROACH

The calculations are carried out with the augmented spherical waves method¹⁷ within the atomic-sphere approximation.¹⁸ The exchange–correlation potential is chosen in the generalized gradient approximation.¹⁹ A dense Brillouin zone (BZ) sampling $30 \times 30 \times 30$ is used. In all calculations the experimental values of the lattice parameters are used (Table I).²⁰ The radii of all atomic spheres are chosen equal.

We describe the interatomic exchange interactions in

terms of the classical Heisenberg Hamiltonian

$$H_{eff} = - \sum_{\mu, \nu} \sum_{\mathbf{R}, \mathbf{R}'} \underset{(\mu \mathbf{R} \neq \nu \mathbf{R}')} J_{\mathbf{R}\mathbf{R}'}^{\mu\nu} \mathbf{s}_{\mathbf{R}}^{\mu} \mathbf{s}_{\mathbf{R}'}^{\nu} \quad (1)$$

In Eq.(1), the indices μ and ν number different sublattices and \mathbf{R} and \mathbf{R}' are the lattice vectors specifying the atoms within sublattices, $\mathbf{s}_{\mathbf{R}}^{\mu}$ is the unit vector pointing in the direction of the magnetic moment at site (μ, \mathbf{R}) . The systems considered contain three 3d atoms in the unit cell with positions $(\frac{1}{4}, \frac{1}{4}, \frac{1}{4})$ for the Mn atom and $(0, 0, 0)$ and $(\frac{1}{2}, \frac{1}{2}, \frac{1}{2})$ for two Ni atoms.

We employ the frozen-magnon approach^{21,22,23} to calculate interatomic Heisenberg exchange parameters. The calculations involve few steps. In the first step, the exchange parameters between the atoms of a given sublattice μ are computed. The calculation is based on the evaluation of the energy of the frozen-magnon configurations defined by the following atomic polar and azimuthal angles

$$\theta_{\mathbf{R}}^{\mu} = \theta, \quad \phi_{\mathbf{R}}^{\mu} = \mathbf{q} \cdot \mathbf{R} + \phi^{\mu}. \quad (2)$$

In the calculation discussed in this paper the constant phase ϕ^{μ} is always chosen equal to zero. The magnetic moments of all other sublattices are kept parallel to the z axis. Within the Heisenberg model (1) the energy of such configuration takes the form

$$E^{\mu\mu}(\theta, \mathbf{q}) = E_0^{\mu\mu}(\theta) + \sin^2 \theta J^{\mu\mu}(\mathbf{q}) \quad (3)$$

where $E_0^{\mu\mu}$ does not depend on \mathbf{q} and the Fourier transform $J^{\mu\nu}(\mathbf{q})$ is defined by

$$J^{\mu\nu}(\mathbf{q}) = \sum_{\mathbf{R}} J_{0\mathbf{R}}^{\mu\nu} \exp(i\mathbf{q} \cdot \mathbf{R}). \quad (4)$$

In the case of $\nu = \mu$ the sum in Eq. (4) does not include $\mathbf{R} = 0$. Calculating $E^{\mu\mu}(\theta, \mathbf{q})$ for a regular \mathbf{q} -mesh in the Brillouin zone of the crystal and performing back Fourier transformation one gets exchange parameters $J_{0\mathbf{R}}^{\mu\mu}$ for sublattice μ .

To determine the exchange interactions between the atoms of two different sublattices μ and ν the frozen-magnon configurations (Eq. 2) are formed for both sublattices. The Heisenberg energy of such configurations takes the form

$$E^{\mu\nu}(\theta, \mathbf{q}) = E_0^{\mu\nu}(\theta) + \sin^2 \theta [J^{\mu\mu}(\mathbf{q}) + J^{\nu\nu}(\mathbf{q})] + 2 \sin^2 \theta \operatorname{Re} J^{\mu\nu}(\mathbf{q}) \quad (5)$$

where $E_0^{\mu\nu}(\theta)$ is a \mathbf{q} -independent part. Performing calculation of $[E^{\mu\nu}(\theta, \mathbf{q}) - E^{\mu\nu}(\theta, \mathbf{0})]$ and subtracting single-sublattice contributions known from the previous step one finds $[\operatorname{Re} J^{\mu\nu}(\mathbf{q}) - \operatorname{Re} J^{\mu\nu}(\mathbf{0})]$. The back Fourier transformation of this expression gives for $\mathbf{R} \neq 0$ the following combinations of the interatomic exchange parameters: $J_{\mathbf{R}}^{\mu\nu} \equiv \frac{1}{2}(J_{0\mathbf{R}}^{\mu\nu} + J_{0(-\mathbf{R})}^{\mu\nu})$. In general, one needs

to perform similar calculations for different phases ϕ^{μ} in Eq. (2) to get another linear combination of the parameters to be able to separate them. For the systems considered these calculations can be avoided by taking into account the symmetry of the lattice (see below).

Quantities $J_{\mathbf{R}}^{\mu\nu}$ does not contain information about the interaction of the atoms within the first unit cell corresponding to $\mathbf{R} = 0$. These exchange parameters can be found in the calculations for magnetic configurations periodic with the periodicity of the lattice. The atoms in the unit cell are separated into two groups. Within each group the moments are parallel. The moments from the different groups form an angle θ . The energies of such magnetic configurations are expressed through the sums $J_0^{\mu\nu} \equiv \sum_{\mathbf{R}} J_{0\mathbf{R}}^{\mu\nu}$. Since the sums $\sum_{\mathbf{R} \neq 0} J_{0\mathbf{R}}^{\mu\nu}$ are known from the preceding step the parameters with $\mathbf{R} = 0$ become accessible. The symmetry relation $J_{00}^{\mu\nu} = J_{0\mathbf{R}}^{\mu\nu}$ for $\mathbf{R} = (0, \frac{1}{2}, \frac{1}{2})$ allows to split the sums $J_{\mathbf{R}}^{\mu\nu}$ to individual parameters.

The Curie temperature is estimated within the mean-field approximation for a multi-sublattice material by solving the system of coupled equations²⁴

$$\langle s^{\mu} \rangle = \frac{2}{3k_B T} \sum_{\nu} J_0^{\mu\nu} \langle s^{\nu} \rangle \quad (6)$$

where $\langle s^{\nu} \rangle$ is the average z component of $\mathbf{s}_{\mathbf{R}}^{\nu}$. Eq. (6) can be represented in the form of eigenvalue matrix problem

$$(\Theta - T\mathbf{I})\mathbf{S} = 0 \quad (7)$$

where $\Theta_{\mu\nu} = \frac{2}{3k_B} J_0^{\mu\nu}$, \mathbf{I} is a unit matrix and \mathbf{S} is the vector of $\langle s^{\nu} \rangle$. The largest eigenvalue of matrix Θ gives the value of Curie temperature.²⁴

III. RESULTS AND DISCUSSION

In Table I we present calculated magnetic moments. For comparison, the available experimental values of the moments and the results of previous calculations are presented. Relative variation of the Mn moment is small. On the other hand, the moment of Ni and X atoms show strong relative variation and are in Ni_2MnSb about two times smaller than in Ni_2MnGa or Ni_2MnIn . The values of the magnetic moments are in good agreement with the results of previous calculations.

The calculated Heisenberg exchange parameters are presented in figure 1. As mentioned in the introduction, the assumption that the closeness of the experimental Curie temperatures is the consequence of the similarity of the exchange interactions is not confirmed by the calculations. We obtain strong dependence of the exchange interactions on the type of the X atom. For X=Ga and X=In that belong to the same column of the Mendellev's table (see inset in Fig. 2) we obtain similar pattern of Heisenberg exchange parameters. On the other hand, for X atoms belonging to different columns the changes

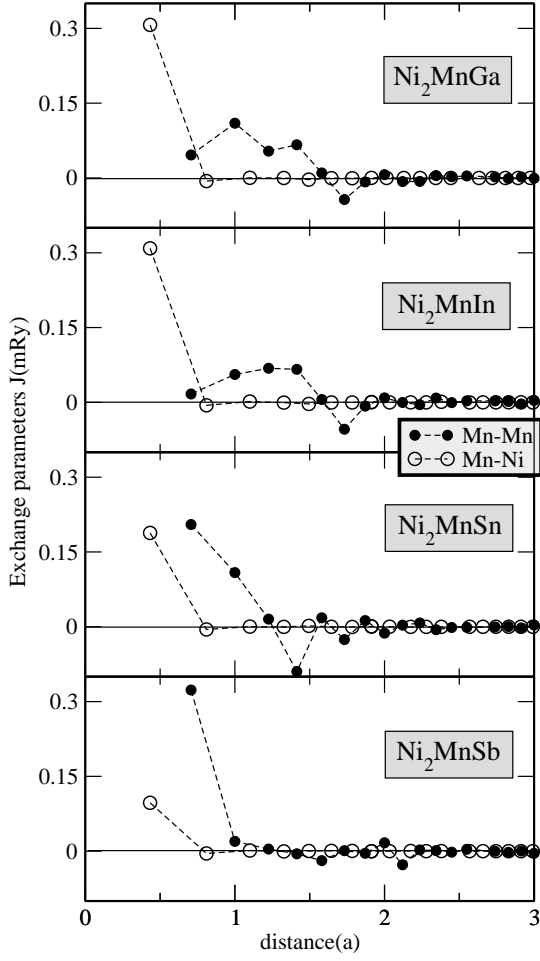


FIG. 1: The parameters of the Mn–Mn (intra-sublattice) exchange interactions and Mn–Ni (inter-sublattice) exchange interactions in Ni_2MnX ($X=\text{Ga, In, Sn, Sb}$). The distances are given in the units of the lattice constant. The significance of the oscillations of the exchange parameters is verified by varying the \mathbf{q} mesh in the frozen-magnon calculations.

in the exchange interactions are very strong (Fig. 1). These changes concern both the Mn–Mn intra-sublattice interactions and the Ni–Mn inter-sublattice interaction.

Considering the Mn–Mn interactions we notice that in Ni_2MnGa and Ni_2MnIn the interaction with the coordination spheres from the first to the fourth is positive. The interaction with the first coordination sphere is weaker than with the following ones. The interaction with the fifth sphere is very small. The interaction with the sixth sphere is negative. The interaction with further coordination spheres is very weak.

In Ni_2MnSn the interaction with the first sphere strongly increases compared with Ni_2MnGa and Ni_2MnIn . On the other hand, the interaction with the third sphere becomes small. The interaction with the fourth sphere is strongly negative. The interaction with further neighbors are weak.

The trend observed in transition from Ni_2MnGa and

TABLE I: Experimental lattice parameters and magnetic moments (in μ_B) of Ni_2MnX ($X=\text{Ga, In, Sn, Sb}$).

	a(a.u.)	Mn	Ni	X	Cell
Ni_2MnGa	11.058 ^a	3.570 (3.43 ^b)	0.294 (0.36 ^b)	-0.068 (-0.04 ^b)	4.090 (4.11 ^b) (4.17 ^c)
Ni_2MnIn	11.468 ^a	3.719	0.277	-0.066	4.208
Ni_2MnSn	11.419 ^a	3.724 (3.53 ^d)	0.206 (0.24 ^d)	-0.057 (-0.03 ^d)	4.080 (4.08 ^d)
Ni_2MnSb	11.345 ^a	3.696	0.143	-0.033	3.950

^aRef.20

^bRef.25

^cRef.26 (Exp.)

^dRef.27

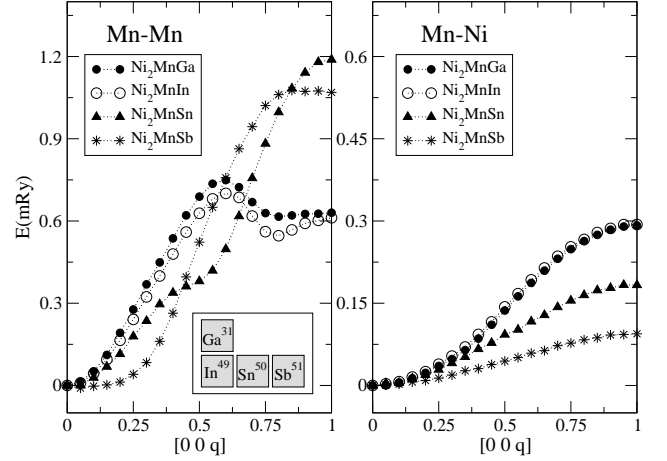


FIG. 2: Frozen-magnon energies as a function of the wave vector \mathbf{q} (in units of $2\pi/a$) in Ni_2MnX for Mn–Mn (left) and Mn–Ni interactions (right).

Ni_2MnIn to Ni_2MnSn becomes even stronger in the case of $X=\text{Sb}$. Here the interaction with the first neighbor increases further and is the only strong exchange interaction between the Mn atoms.

The inter-sublattice Mn–Ni interaction behaves very differently. A sizable interaction takes place only between nearest neighbors. This interaction is very strong in Ni_2MnGa and Ni_2MnIn and quickly decreases for $X=\text{Sn}$ and, especially, $X=\text{Sb}$.

To reveal the physical origin of the strong difference in the exchange parameters of these systems we plot in Fig. 2 the frozen-magnon energies as a function of wave vector \mathbf{q} for one direction in the Brillouin zone.²⁸ We remind the reader that the inter-atomic exchange parameters are Fourier transforms of the $E(\mathbf{q})$ functions and therefore reflect their form. Indeed, $E(\mathbf{q})$ curves for Ni_2MnGa and Ni_2MnIn are close to each other that leads to a similar set of interatomic exchange parameters (Fig. 1). These curves deviate strongly from a simple cosinusoid having a maximum at \mathbf{q} about 0.6 and a rather weak variation

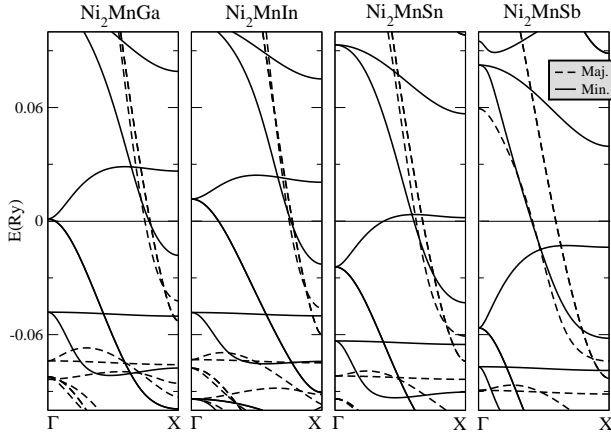


FIG. 3: Band structure of Ni_2MnX along the high symmetry line (Γ -X).

at $\mathbf{q} > 0.6$.²⁹ The complexity of $E(\mathbf{q})$ means that several Fourier components are needed to describe the features of the function. This is reflected in the Heisenberg's parameters of Ni_2MnGa and Ni_2MnIn .

On the other hand, the $E(\mathbf{q})$ curve of Ni_2MnSb is well described by one cosinusoid (Fig. 2) that results in a single large Mn-Mn exchange parameter (Fig. 1). The $E(\mathbf{q})$ of Ni_2MnSn assumes an intermediate position from the viewpoint of the complexity of the function. This property is also reflected in the exchange parameters (Fig. 1).

Note that the character of the \mathbf{q} -dependence of the energy illustrated by Fig. 2 is a consequence of the properties of the electronic structure of the compounds. Indeed, in Fig. 3 we see that the electronic structures of Ni_2MnGa and Ni_2MnIn are similar. Transition along the row In-Sn-Sb leads to increasing difference in the electron spectrum. This increasing difference can be traced back to the change in the number of valence electrons: a Sb atoms has two more valence electrons than In and one more electron than Sn. As the result an important difference in the electron structure of the system is a relative shift of the Fermi level to a higher energy position in the sequence In-Sn-Sb. This shift is clearly seen in the DOS presented in Fig. 4. The positions of the same features of the DOS in different systems are well described by linear functions with negative angle coefficients. For the Mn peaks all three lines are almost parallel. This means that the change in the Mn DOS from system to system can be treated as a rigid shift with respect to the Fermi level. In the case of the Ni-DOS the situation is more complicated since, besides the variation of the electron number, an additional influence on the peak positions is exerted by the variation of the Ni atomic moment (see Table I).

The $E(\mathbf{q})$ curves determining the Mn-Ni interactions are presented in Fig. 2. The form of the curves is in all cases close to a cosinusoid. Therefore, only one exchange parameter has sizable value. The strength of the interaction is in correlation with the value of the magnetic

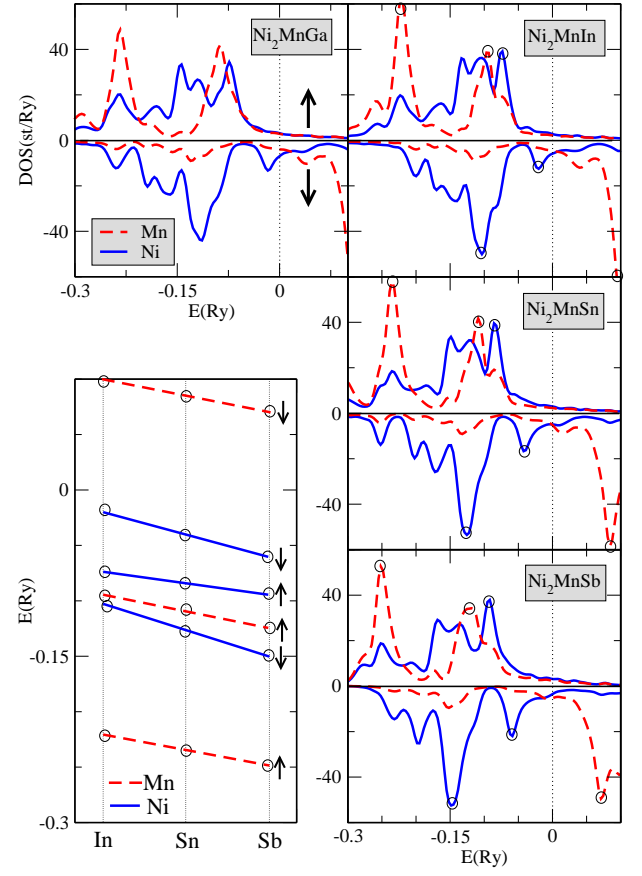


FIG. 4: Spin-projected partial density of states of Ni_2MnX . The separate graph in the left-hand bottom part of the figure shows the variation of the positions of a number of the DOS peaks for the In-Sn-Sb series of compounds. The lines in this graph are guides for the eye. The energies are measured with respect to the Fermi level of the corresponding system. The small open circles on the DOS curves mark the positions of the peaks. Arrows show spin projections. The analysis of the states at the Fermi level shows that the main contributions come from the 3d states of Mn and Ni.

TABLE II: Mean-field estimation of the Curie temperatures for Ni_2MnX ($X=\text{Ga}, \text{In}, \text{Sn}, \text{Sb}$). The experimental Curie temperature values are taken from Ref.20.

	$T_c^{Mn-Mn[MFA]}(K)$	$T_c^{[MFA]}(K)$	$T_c^{[Exp]}(K)$
Ni_2MnGa	302	389	380
Ni_2MnIn	244	343	315
Ni_2MnSn	323	358	360
Ni_2MnSb	343	352	365

moment of the Ni atoms.

The interatomic exchange parameters are used to evaluate the Curie temperature. If only the Mn-Mn interactions are taken into account we obtain values shown in Table II. Despite very strong difference in the Mn-Mn exchange parameters in these systems the difference in

the corresponding Curie temperatures is not very large. The explanation for this result is the property that in MFA to a one-sublattice ferromagnet the value of the Curie temperature is determined by the sum of the interatomic exchange interactions $J_0 = \sum_{\mathbf{R} \neq 0} J_{0\mathbf{R}}$. J_0 gives the average value of $E(\mathbf{q})$ and is less sensitive to the detailed form of the $E(\mathbf{q})$ function.

The comparison of the Curie temperatures calculated with the use of the Mn–Mn exchange parameters only with experimental Curie temperatures shows that the agreement with experiment is not in general good. In the case of Ni_2MnGa the error is about 30%.

Account for inter-sublattice interactions improves the agreement with experimental T_C values considerably (Table II). This shows that the Ni moment provides a magnetic degree of freedom which plays important role in the thermodynamics of the system.

IV. CONCLUSION

In conclusion, we have systematically studied exchange interactions and Curie temperatures in Ni–based full

Heusler alloys Ni_2MnX ($X = \text{Ga, In, Sn, Sb}$) within the parameter-free density functional theory. Our calculations show that despite similarity of the Curie temperatures of these systems there is strong difference in the underlying magnetic interactions. This difference involves both the Mn–Mn and Mn–Ni exchange interactions which depend strongly on the X constituent. The Curie temperatures are calculated within the mean-field approximation to the classical Heisenberg Hamiltonian by solving a matrix equation for a multi-sublattice system. Good agreement with experiment for all four systems is obtained.

Acknowledgments

The financial support of Bundesministerium für Bildung und Forschung is acknowledged.

-
- ¹ H. Ohno, Science **281**, 951 (1998).
 - ² R. A. de Groot, F. M. Mueller, P. G. van Engen and K. H. J. Buschow, Phys. Rev. Lett. **50**, 2024 (1983).
 - ³ I. Galanakis, P. H. Dederichs, and N. Papanikolaou Phys. Rev. B **66**, 174429 (2002).
 - ⁴ K. A. Kilian, R. H. Victora J. Appl. Phys. **87**, 7064
 - ⁵ J. Q. Xie, J. W. Dong, Lu J, C. J. Palmstrm and S. McKernan, Appl. Phys. Lett. **79**, 1003 (2001).
 - ⁶ M. Kurfiss and R. Anton, J. Alloy. Comp. **361**, 36 (2003).
 - ⁷ P. J. Webster, K. R. A. Ziebeck, S. L. Town, and M.S. Peak, Philos. Mag. **49**, 295 (1984).
 - ⁸ L. Ritchie, G. Xiao, Y. Ji, T. Y. Chen, C. L. Chien, M. Zhang, J. Chen, Z. Liu, G. Wu, and X. X. Zhang, Phys. Rev. B **68**, 104430 (2003).
 - ⁹ M. P. Raphael, B. Ravel, M. A. Willard, S. F. Cheng, B. N. Das, R. M. Stroud, K. M. Bussmann, J. H. Claassen, and V. G. Harris, Appl. Phys. Lett. **79**, 4396 (2001).
 - ¹⁰ S. Picozzi, A. Continenza, and A. J. Freeman Phys. Rev. B **66**, 094421 (2002).
 - ¹¹ S. Plogmann, T. Schlathölter, J. Braun, M. Newmann, Y. M. Yarmoshenko, M. Yablonskikh, E. I. Shreder, E. Z. Kurmaev, A. Wrona, and A. Slebarski, Phys. Rev. B **60**, 6428 (1999).
 - ¹² J. Kübler Phys. Rev. B **67**, 220403 (2003).
 - ¹³ G. A. de Wijs and R. A. de Groot Phys. Rev. B **64**, 020402 (2001).
 - ¹⁴ M. P. Raphael, B. Ravel, Q. Huang, M. A. Willard, S. F. Cheng, B. N. Das, R. M. Stroud, K. M. Bussmann, J. H. Claassen, and V. G. Harris, Phys. Rev. B **66**, 104429 (2002).
 - ¹⁵ J. Kübler, A. R. Williams, and C. B. Sommers, Phys. Rev. B **28**, 1745(1983).
 - ¹⁶ J. Enkovaara, A. Ayuela, J. Jalkanen, L. Nordström, and R.M. Nieminen, Phys. Rev. B **67**, 054417 (2003).
 - ¹⁷ A. R. Williams, J. Kübler, and C. D. Gelatt, Phys. Rev. B **19**, 6094(1979).
 - ¹⁸ O. K. Andersen, Phys. Rev. B **12**, 3060 (1975).
 - ¹⁹ J. P. Perdew and Y. Wang, Phys. Rev. B **45**, 13244 (1992).
 - ²⁰ P. J. Webster and K. R. A. Ziebeck, in *Alloys and Compounds of d-Elements with Main Group Elements*, Part 2, edited by H. R. J. Wijn, Landolt-Börnstein, New Series, Group III, Vol. 19/c (Springer, Berlin, 1988), pp. 75-184.
 - ²¹ N. M. Rosengaard and B. Johansson, Phys. Rev. B **55**, 14975 (1997).
 - ²² S. V. Halilov, H. Eschrig, A. Ya. Perlov, and P. M. Oppeneer, Phys. Rev. B **58**, 293 (1998).
 - ²³ L. M. Sandratskii and P. Bruno, Phys. Rev. B **67**, 214402 (2003).
 - ²⁴ P. W. Anderson, *Theory of magnetic exchange interactions: Exchange in insulators and semiconductors*, in *Solid State Physics*, Edited by F. Seitz and Turnbull (Academic Press, New York), Vol. 14 pp. 99-214.
 - ²⁵ A. Ayuela, J. Enkovaara and R.M. Nieminen, J. Phys.: Condens. Matter **14**, 5325 (2002).
 - ²⁶ J. Worgull, E. Petti, and J. Trivisonno, Phys. Rev. B **54**, 15695 (1996).
 - ²⁷ A. Ayuela, J. Enkovaara, K. Ullakko and R.M. Nieminen, J. Phys.: Condens. Matter **11**, 2017 (1999).
 - ²⁸ The energy of the frozen magnon with a given \mathbf{q} can be seen as a result of a complex interaction of the ferromagnetic states separated by vector \mathbf{q} in the reciprocal space [L. M. Sandratskii, Adv. Phys. **47**, 1 (1998)]. This interaction is stronger if the states have close energies and weaker for the states separated by a large energy interval. Note that the DOS is an integrated characteristic and does not contain information about the distribution of the states in the reciprocal space. Therefore the study of the DOS is not sufficient for understanding of the character of the \mathbf{q}

dependence of the frozen-magnon dispersion.

- ²⁹ Recently Bungaro et al [C. Bungaro, K.M. Rabe, and A.D. Corso, Phys. Rev. B **68**, 134104 (2003)] reported calculation of the phonon dispersion in Ni₂MnGa and found a nonmonotonous behaviour qualitatively similar to the behaviour obtained by us for the frozen-magnon dispersion of Ni₂MnGa and Ni₂MnIn (Fig.2). They also studied the properties of the Fermi surface and discussed the absence

of the coupling of the nesting parts of the Fermi surface to the phonons. The features of the Fermi surface can be important for formation the details of the frozen-magnon dispersions such as the maximum at $\mathbf{q} \sim 0.6$ for Ni₂MnGa and Ni₂MnIn. Our calculations show, however, that the ground state is ferromagnetic. No instability connected with formation of a spin-density wave ground state is detected.